JOURNAL OF VIROLOGY, Feb. 2003, p. 2615–2622 Vol. 77, No. 4
0022-538X/03/$08.00+0 DOI: 10.1128/JVI.77.4.2615–2622.2003

Cell Penetration and Trafficking of Polyomavirus

Joanna M. Gilbert,[1]* Ilya G. Goldberg,[2]† and Thomas L. Benjamin[1]

Department of Pathology, Harvard Medical School, Boston, Massachusetts 02115,[1] and Department of Biology, Massachusetts Institute of Technology, Cambridge, Massachusetts 02139[2]

Received 15 August 2002/Accepted 18 September 2002

The murine polyomavirus (Py) enters mouse fibroblasts and kidney epithelial cells via an endocytic pathway that is caveola-independent (as well as clathrin-independent). In contrast, uptake of simian virus 40 into the same cells is dependent on caveola. Following the initial uptake of Py, both microtubules and microfilaments play roles in trafficking of the virus to the nucleus. Colcemid, which disrupts microtubules, inhibits the ability of Py to reach the nucleus and replicate. Paclitaxel, which stabilizes microtubules and prevents microtubule turnover, has no effect, indicating that intact but not dynamic microtubules are required for Py infectivity. Compounds that disrupt actin filaments enhance Py uptake while stabilization of actin filaments impedes Py infection. Virus particles are seen in association with actin in cells treated with microfilament-disrupting or filament-stabilizing agents at levels comparable to those in untreated cells, suggesting that a dynamic state of the microfilament system is important for Py infectivity.

Genetically and structurally related small nonenveloped DNA viruses of the *Polyomaviridae* infect different species and have different cell tropisms within their respective hosts. Recent studies have indicated considerable diversity in the early steps of infection by different members of this group. Simian virus 40 (SV40) binds to major histocompatibility complex class I as its primary receptor (2), and its attachment is not dependent on cell surface sialic acid. The mouse polyomavirus (Py) does not depend on major histocompatibility complex class I (38) but rather on a possibly diverse class of glycoproteins that carry sialic acid in an α-2,3 linkage as an essential feature (4, 10, 14). The attachment of JC virus (JCV) to glial cells is also sialic acid dependent but requires an α-2,6 linkage of the sugar (23).

Early electron microscopic studies suggested that Py and SV40 might enter cells in a similar fashion. Immediately after uptake, single particles are seen within small, apparently uncoated vesicles (15, 24, 26). Multiple virus particles are occasionally seen in larger vesicles and, after longer incubation, in tubular membrane-bounded structures that were possibly derived from the endoplasmic reticulum (ER) (13, 15, 17, 24, 26, 27). More-recent results, however, have indicated that these viruses use different modes to penetrate their host cells. Utilization of caveola by SV40 in entry into CV-1 cells was first reported by Anderson et al. (1) and subsequently confirmed by others (33, 44). Caveola-derived vesicles containing SV40 traffic to an organelle termed a caveosome (32) prior to reaching tubules derived from the smooth ER. SV40 particles appear to undergo partial dissociation in these ER-derived tubules before reaching the nucleus (31).

Experiments regarding the uptake of Py have so far not given uniform results with respect to dependence on caveola (11, 36). In one study, Py was found to enter murine fibroblasts (NIH 3T3 cells) or primary baby mouse kidney (BMK) epithelial cells by using small, uncoated vesicles that were neither caveola nor clathrin coated, since disruption of either endocytic pathway had no effect on virus entry (11). An independent study which used different host cells and a different pharmacological agent to disrupt caveolae concluded that caveolae are required for Py entry (36). In contrast to both SV40 and Py, JCV enters glial cells by clathrin-mediated endocytosis (34). Cell attachment is not necessarily followed by uptake and infection, however, as indicated by studies of JCV and its interaction with B cells (47, 49).

Studies have begun to address how these viruses, once internalized in vesicles, are conveyed to sites of uncoating and eventually reach the nucleus and the roles of cytoskeletal elements in these processes. Disruption of the microtubule network, but not of actin microfilaments, was shown to inhibit SV40 infectivity (39). Microtubules are required for the transport of SV40-containing vesicles from the caveosome to perinuclear, smooth ER-derived tubules (32). In a recent study, a role for actin was demonstrated in the uptake of SV40 in a dynamin-dependent process (33). Interestingly, a dominant-negative form of dynamin I, which inhibits the uptake of both caveola-derived and clathrin-coated vesicles, was found not to inhibit the entry of Py into NIH 3T3 cells (11). In one study, actin filaments were also found not to be required for Py infectivity, whereas microtubules were (20). However, in another study, the association of Py with both microtubules and actin filaments was observed (36). These contrasting results on the uptake of Py versus SV40 raise questions as to whether the mechanism of cell entry is entirely intrinsic to a particular virus or may be dictated in part by the host cell.

The same question may be raised concerning the unusually broad tropism of Py in its natural host, where it infects more than 30 distinct cell types of both epithelial and mesenchymal origin (8). It induces tumors in a wide variety of tissues in the mouse and efficiently transforms heterologous cells in culture

* Corresponding author. Mailing address: Department of Pathology, Harvard Medical School, 200 Longwood Ave., Armenise-233, Boston, MA 02115. Phone: (617) 432-1998. Fax: (617) 432-2689. E-mail: jgilbert@hms.harvard.edu.

† Present address: Laboratory of Genetics, National Institute on Aging, NIH, Baltimore, MD 21224.

derived from rats or hamsters. Its ability to infect a wide range of cell types is based in part on the binding of the major viral capsid protein VP1 to sialyloligosaccharides, which are abundantly expressed on the surfaces of many cells (3, 8, 45), but also on the ability to penetrate, uncoat, and reach the nucleus in each of its target cells. The extent to which the virus depends on the same cellular machinery and pathways to penetrate and traffic in each of its target cells is unknown.

MATERIALS AND METHODS

Cells and viruses. Primary BMK cells were prepared and used 3 to 4 days after plating. NIH 3T3 and CV-1 cells were purchased from the American Type Culture Collection. Cells were maintained in Dulbecco's modified Eagle's medium (DMEM; Sigma Chemical Company, St. Louis, Mo.) containing 4.5 g of glucose per liter, 10% heat-inactivated calf serum (CS; Life Technologies, Gaithersberg, Md.), 100 IU of penicillin per ml, and 100 IU of streptomycin (Life Technologies) per ml in a 5% CO_2 humidified incubator at 37°C.

The Py strain RA (small plaque strain) was propagated on BMK cells. The virus was twice purified by CsCl equilibrium centrifugation as previously described (6, 28). The viral protein concentration was determined by the MicroBCA assay (Pierce Chemical Company, Rockford, Ill.) and by the optical density at 280 nm (OD_{280})/OD_{260} ratio. The titers of the virus were determined by plaque assay. Purified Py was labeled with the FluoReporter Oregon green 488 protein labeling kit (Molecular Probes, Eugene, Oreg.) according to the manufacturer's instructions as described by Gilbert and Benjamin (11). By plaque assay titration and OD, the infectious-to-physical particle ratio of Oregon green-labeled Py (OGPy) was determined to be approximately 1 to 7.5.

SV40 (strain 777) was propagated on CV-1 cells. The titers of the virus were determined by plaque assay on CV-1 cells.

Antibodies and reagents. 4′,6′-diamidino-2-phenylindole (DAPI), paclitaxel, cytochalasin B (cyto B), cyto D, methyl-β-cyclodextrin (MβCD), and the monoclonal antibody clone B-5-1-2 against α-tubulin were purchased from Sigma. Colcemid, jasplakinolide (jas), nystatin, latrunculin A (lat A), lat B, and the antibody to SV40 large T antigen (LTAg) (clone Ab-2) were purchased from Calbiochem (San Diego, Calif.). BODIPY TR-X phallacidin, Oregon green-conjugated goat anti-rat or anti-mouse immunoglobulin G and rhodamine-conjugated goat anti-mouse immunoglobulin G were purchased from Molecular Probes. The rat monoclonal antibody to Py LTAg and the rabbit polyclonal antibody to the major capsid protein of Py, VP1, were generated within the lab.

Indirect immunofluorescence assay (IFA). After a desired incubation time, cells were fixed in 4% paraformaldehyde (Electron Microscopy Sciences, Ft. Washington, Pa.). Samples were permeabilized by incubation in either ethanol-acetic acid (2:1) for examination of Py LTAg or 0.5% Triton X-100 with 5% CS in phosphate-buffered saline for examination of all other antibodies used as well as for the TR-X phallacidin. Samples were incubated with the primary antibody in 1% CS, with or without 0.1% Triton X-100, for 1 h at room temperature (RT). Samples were incubated with either Oregon green- or rhodamine-labeled secondary antibodies and DAPI and incubated for 1 h at RT or for 20 min at RT for TR-X phallacidin. The washed coverslips were mounted with Moviol, sealed with nail polish, and examined by standard fluorescence microscopy with a Nikon Eclipse microscope with an apochromatic Plan 60×/1.4 oil objective. For deconvolution microscopy (48), data were collected with a Nikon Eclipse microscope with an apochromatic Plan 100×/1.4 oil objective equipped with a Delta Vision optical sectioning system employing SoftWoRx software (Applied Precision, Inc., Issaquah, Wash.) with 0.2-μm-thick step Z sections. The deconvolved images were saved as TIFFs and then imported and prepared in Adobe Photoshop 6.

For both BMK and NIH 3T3 cells, 100 μg of nystatin per ml and 7.5 mM MβCD were used. The concentrations of Colcemid used were 600 ng per ml for BMK cells and 1,200 ng per ml for NIH 3T3 cells. The paclitaxel concentrations used were either 1 or 10 μM for either BMK or NIH 3T3 cells. Cells were treated with the following concentrations of the indicated compounds to disrupt actin without causing the cells to completely round up. The concentrations used to disrupt actin for cyto B and D and for lat A and B disruption of the actin cytoskeleton were 6 μM cyto B, 1.2 μM cyto D, 1 μM lat A, and 0.5 μM lat B for BMK cells. The concentrations used for NIH 3T3 cells were 6 μM cyto B, 0.6 μM for cyto D, 0.1 μM lat A, and 0.5 μM lat B. BMK and NIH 3T3 cells were treated with 10 and 25 nM jas, respectively; the concentration that showed increased fluorescence with TR-X phallacidin was compared to that of the untreated control. The concentrations of the compounds used did not appear to be cytotoxic during these studies, with the exception of MβCD (see Results).

Infectivity assay. For analysis of Py infectivity, cells were plated on 12-mm-diameter glass coverslips and grown to approximately 80% confluency at 37°C in a CO_2 incubator in 24-well dishes. Cells were pretreated or not with the various compounds described above, as indicated. Cells were chilled on ice and infected with ice-cold, plaque-titered stocks of Py (RA strain; dilutions ranging from a multiplicity of infection [MOI] of 1 to 100, as indicated) or SV40 (777 strain; an MOI of 10) diluted in DMEM without bicarbonate (HCO_3^-) containing 2% CS and buffered with 10 mM HEPES (pH 5.4), with or without the indicated compounds. The samples were incubated with cells for 1 h at 4°C. Unbound virus was removed by aspiration, cells were rinsed with cold DMEM containing 2% CS with HCO_3^-, prewarmed media, with or without compounds, was added, and the samples were incubated at 37°C in a CO_2 incubator for the indicated amount of time. Where indicated, extracellular virus was neutralized by the addition of an anti-VP1 antibody in DMEM with 2% CS, with or without the indicated compounds. Py was allowed to replicate for 24 h for BMK cells or 36 h for NIH 3T3 cells at 37°C. SV40 and Py infections were allowed to replicate for 32 h in both NIH 3T3 and BMK cells. Successful entry was assessed by nuclear expression of Py LTAg by IFA, as described above. Data are presented as the percentages of nuclei that were LTAg positive in the treated sample relative to the percent LTAg positive in the untreated control. Values are presented as the averages of duplicate samples where approximately 500 nuclei were counted per sample.

Colocalization assay. To assess entry and colocalization of fluorescently labeled Py, OGPy was diluted in DMEM–2% CS without HCO_3^- and added to prechilled cells that had been pretreated or not with compounds as indicated. Virus was allowed to bind for 60 min at 4°C. Unbound virus was removed by aspiration, and cells were rinsed with cold DMEM–2% CS with HCO_3^-. Prewarmed media, with or without compounds, was added, and then samples were incubated at 37°C in a CO_2 incubator for the indicated amount of time. Samples were then fixed in 4% paraformaldehyde at the indicated times and processed by IFA as described above. Each experiment was performed three times, and from each experiment, at each time point, three random fields were imaged and then the Z stacks were subjected to deconvolution (48). Each individual deconvolved Z section was examined for the number of OGPy particles and the number of OGPy particles colocalized with either microtubules or actin.

RESULTS

The effect of caveolae-disrupting drugs on Py and SV40 infectivity. Previous studies indicated that Py enters established murine fibroblasts (NIH 3T3) and primary BMK epithelial cells in a caveola-independent and clathrin-independent process (11). A separate study utilizing different cells (3T6 fibroblasts and NMuMG [murine mammary epithelial cells]) and a different compound to inhibit caveolae showed a dependence of Py uptake on caveolae (36). Several studies have shown that SV40 is taken into primate cells via caveolae (1, 33, 44). NIH 3T3 and BMK cells can serve as common hosts for SV40 and Py, with the former giving a nonproductive infection leading to transformation and the latter giving a productive cytocidal infection. These cells thus offer the possibility to test whether Py and SV40 utilize the same or different pathways of entry in a common host and to rule out differences being due to different pharmacological agents used in previous studies. Cholesterol-binding compounds can disrupt lipid rafts and interfere with uptake via caveolae (reviewed in reference 41). NIH 3T3 and BMK cells were pretreated either with the cholesterol-sequestering compound nystatin or the cholesterol-depleting compound MβCD for 1 h at 37°C followed by infection with SV40 or Py. The ability of the viruses to penetrate the cells and initiate infection was measured by expression of the respective viral LTAgs in the nucleus by indirect immunofluorescence. The results in Table 1 show that infection by SV40 was reduced five- to eightfold in nystatin-treated and three- to fourfold in MβCD-treated cells compared to untreated controls. Infection by Py was unaffected by either drug. Higher concentrations of MβCD were cytotoxic. The results for the

TABLE 1. Effect of caveolae-disrupting compounds on infectivity

Treatment	% LTAg-positive nuclei in virus-infected cells			
	BMK		NIH 3T3	
	SV40	Py	SV40	Py
None (control)	100	100	100	100
Nystatin	22	98	12	108
MβCD	24	103	30	94

two viruses were substantially the same in the two cell types tested. These results confirm and extend those reported earlier indicating that SV40 requires functional caveolae for infection, whereas Py, at least in some mouse cells, does not (1, 11, 33, 44).

The role of microtubules in Py infectivity. To determine whether microtubules are required for Py infection, NIH 3T3 and BMK cells were mock treated or pretreated with either the microtubule-disrupting agent Colcemid or the microtubule-stabilizing agent paclitaxel. After treatment, cells were infected and incubated in the continued presence of the drugs for 24 to 32 h. Cells were then fixed and stained for the expression of Py LTAg by immunofluorescence. Sharp reductions in infection of both BMK and NIH 3T3 cells were seen when cells were treated with Colcemid compared with mock-treated control cells (Table 2). Inhibition of Py infectivity by Colcemid was shown to be independent of the MOI over a broad range (1 to 100 PFU/cell) in both cell types (data not shown). In contrast, when cells were treated with the microtubule-stabilizing agent paclitaxel (either 1 or 10 μm), there was no effect on Py infectivity (Table 2). These results indicate that infection by Py requires intact microtubules but does not depend on dynamic aspects of microtubule function.

Kinetics of microtubule disruption and Py infectivity. To determine the stage in virus entry at which microtubules are required, Colcemid was added at various times postinfection and left in until assayed for Py LTAg expression. Colcemid disruption of the microtubule network in BMK cells as late as 6 h postinfection diminished Py infectivity by 50% (Fig. 1). After 8 h, microtubule disruption no longer inhibited Py infection. Results with NIH 3T3 cells were similar, except that the Colcemid-sensitive period was longer, extending to between 12 and 16 h. Microtubules are not required for viral particles to be endocytosed from the cell surface, as experiments with and without neutralizing antibody showed no difference in the efficiency or kinetics of uptake (data not shown).

Colocalization of Py and microtubules. Since Py requires intact microtubules for infectivity, the ability of the virus to colocalize with microtubules was examined. Purified Py was

TABLE 2. Effect of microtubule-interacting compounds on Py infectivity

Treatment	% Py LTAg-positive nuclei in cell type	
	BMK	NIH 3T3
None (control)	100	100
Colcemid	9	4
Paclitaxel	97	92

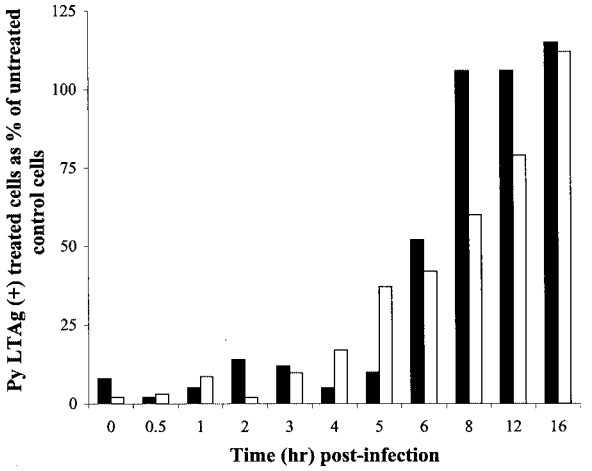

FIG. 1. Effect of Colcemid addition on infectivity of BMK and NIH 3T3 cells. Cells were infected with Py, and control medium or medium containing Colcemid was added at the indicated time points postinfection. Cells were examined for Py LTAg staining at either 24 h for BMK cells or 36 h for NIH 3T3 cells. Approximately 500 nuclei were counted per sample. Results are presented as the percentages of nuclei that were Py LTAg positive in the treated sample relative to the percent positive in the untreated control. Black bars represent Colcemid-treated BMK cells, and white bars represent Colcemid-treated NIH 3T3 cells.

labeled with the fluorophore Oregon green as previously described (11) and used to infect BMK cells with or without Colcemid. Cells and OGPy were incubated for various times at 37°C in the continued presence of Colcemid or left untreated. Cells were then fixed, processed for immunological detection of tubulin, and examined by fluorescence microscopy, and the micrographs were subjected to deconvolution. Individual Z sections of the deconvolved images were examined for colocalization of OGPy and tubulin. At 3 h postinfection, multiple virions were seen to localize with microtubules in untreated cells, but very few were seen to interact with tubulin after disruption with Colcemid (Fig. 2). Similar colocalization with tubulin was seen in untreated NIH 3T3 cells (data not shown). The quantitation and kinetics of this interaction between OGPy and microtubules in BMK cells are shown in Fig. 3. The percentage of OGPy particles interacting with tubulin in untreated cells increased with time, reaching maximal levels at 3 to 4 h postinfection, and decreased thereafter (Fig. 3). Much lower levels of OGPy colocalizing with tubulin were seen in Colcemid-treated cells. These data indicate that vesicles containing Py (or the Py particles themselves) interact with intact microtubules and, to a significantly lesser extent, with disrupted microtubules. The kinetics of interaction of Py with intact microtubules is consistent with the period of Colcemid sensitivity shown in Fig. 1.

Role of the actin cytoskeleton in Py infectivity. To determine whether the actin cytoskeleton is required for Py infectivity, the effect of disrupting actin microfilaments was examined. BMK and NIH 3T3 cells were mock treated or pretreated and infected in the presence of either the f-actin-disrupting compounds cyto B and D, the g-actin-sequestering compounds lat A and B, or the actin filament-stabilizing compound jas. Cells were left in the presence of these compounds until they were

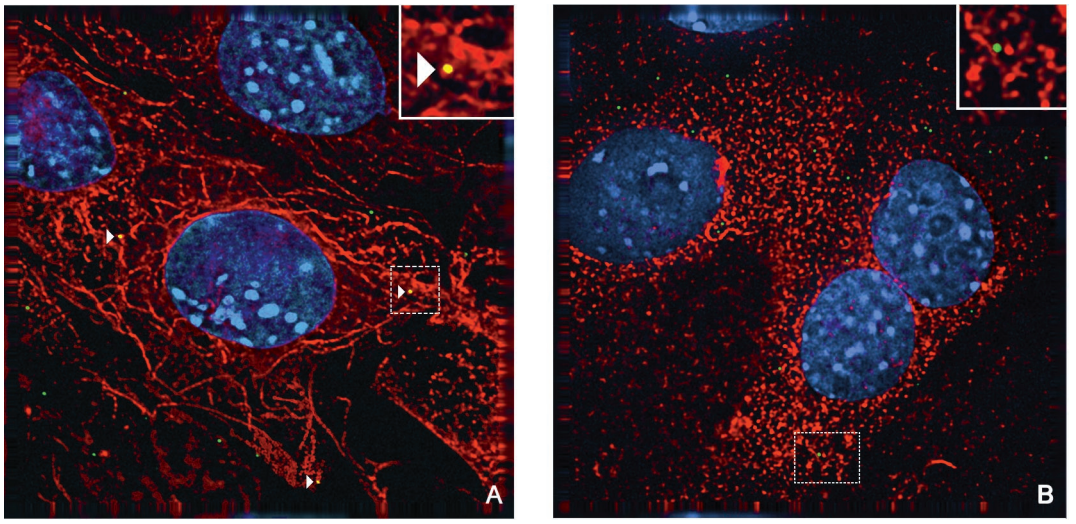

FIG. 2. Colocalization of OGPy with microtubules. BMK cells were mock treated or pretreated with Colcemid. Cells were infected with OGPy in the absence (A) or presence (B) of Colcemid and then incubated further with or without Colcemid. Cells were fixed, processed for immunodetection of tubulin, imaged, and then subjected to deconvolution. Z sections (0.2 μm thick) were examined, and representative sections showing cells that were incubated for 3 h at 37°C prior to fixation are presented. Colocalized OGPy particles are indicated with white arrowheads.

fixed and examined for expression of Py LTAg. All four of the actin-disrupting compounds increased Py infectivity in both BMK and NIH 3T3 cells (Table 3). In contrast, stabilization of actin filaments by the addition of jas decreased the efficiency of infection in both BMK and NIH 3T3 cells (Table 3). These results suggest that Py does not depend on preexisting stable microfilaments but rather on some dynamic aspect of microfilament assembly and disassembly.

To determine the kinetics of the effects of the various actin-binding drugs on virus entry, lat A, cyto B, or jas was added 1 h prior to infection and washed out concurrent with neutralization of extracellular virus at various times after infection. Results are shown in Fig. 4 for BMK cells and in Fig. 5 for NIH 3T3 cells. When lat A or cyto B was present through the first 0.5 h postinfection, increases of 2.5- to 3.5-fold in infectivity were seen compared to untreated cells. Thus, disruption of actin microfilaments very early in infection enhances the uptake of Py, leading to greater infectivity. The enhancement effect of microfilament disruption on Py infectivity is observed at moderate MOIs (10 to 20 PFU/cell) and is not evident at very high MOIs (data not shown).

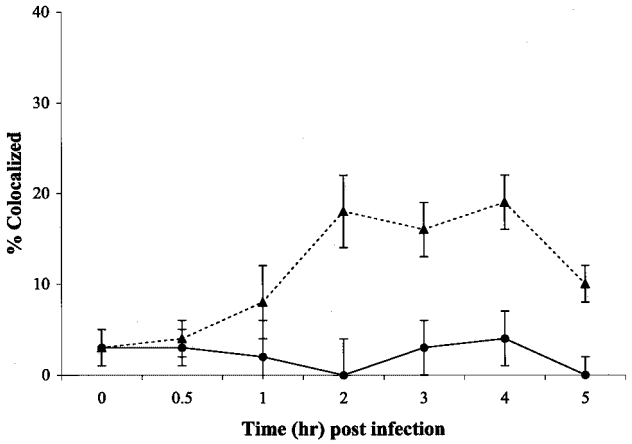

FIG. 3. Quantitation of colocalization of microtubules and OGPy. BMK cells were mock treated (▲) or pretreated with Colcemid (●) and then infected with OGPy in the presence or absence of Colcemid. Samples were fixed and processed for immunodetection of tubulin. After deconvolution, each individual 0.2-μm-thick Z section was examined for total virus particles and particles colocalized with tubulin. The averages of three randomly selected fields from three experiments were taken for each time point.

When microfilament turnover was inhibited by adding jas prior to and during the first several hours postinfection, Py infectivity was reduced two- to threefold. This inhibition was evident in both BMK and NIH 3T3 cells (Fig. 4 and 5). The inhibitory effect of jas disappears by 4 to 5 h postinfection. These results indicate that a dynamic state of actin microfilaments promotes some early step of Py entry and that blocking microfilament turnover has a transient inhibitory effect.

Colocalization of Py and actin. Cells were examined microscopically to determine if there is an interaction between Py and the actin cytoskeleton in the presence and absence of drugs. BMK cells were untreated, pretreated with lat A or jas, and infected with OGPy. At the indicated times, cells were fixed, processed for detection of actin, examined by fluorescence microscopy, and subjected to deconvolution. Individual

TABLE 3. Effect of actin-interacting compounds on Py infectivity

Treatment	% Py LTAg-positive nuclei	
	BMK	NIH 3T3
None (control)	100	100
Lat A	309	172
Lat B	236	155
Cyto B	218	169
Cyto D	209	159
Jas	55	52

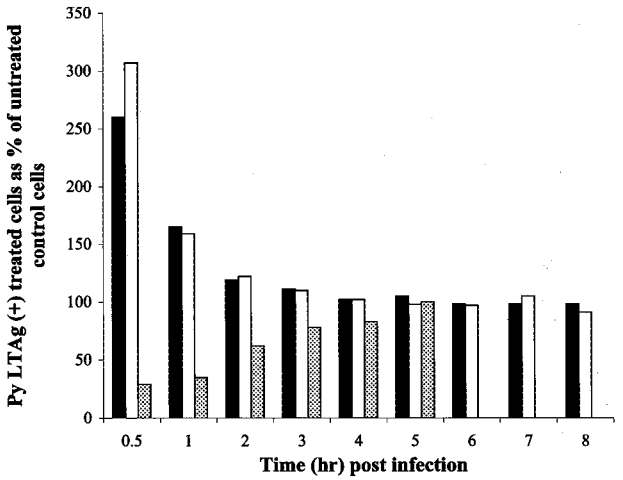

FIG. 4. Effect of actin binding compounds on BMK cells. BMK cells were pretreated with media alone or media containing either lat A (black bars), cyto B (white bars), or jas (dotted bars). Cells were infected with Py (at an MOI of 10) for 1 h in media alone or media containing the above compounds. The compounds were washed out, and neutralizing antibody was added at the indicated time points. Cells were examined for Py LTAg staining at 24 h. Approximately 500 nuclei were counted per sample, and the data are presented as described in the legend to Fig. 1.

Z sections of the deconvolved images were examined for colocalization of OGPy and actin. Very few virions were seen to localize with actin filaments in untreated BMK cells 30 min postinfection, indicating possible transient association of virus with microfilaments (Fig. 6A). In BMK cells in which the actin cytoskeleton was disrupted with lat A, OGPy particles were seen more frequently associated with actin (Fig. 6B). Similar colocalization was seen with the other actin-disrupting compounds and also in Py-infected NIH 3T3 cells (data not shown). Interestingly, OGPy particles were also seen to colocalize with actin in jas-treated BMK cells (Fig. 6C). Quantitation of these data revealed an increase in colocalization of OGPy with actin in lat A-treated cells, reaching a maximal level at 0.5 h postinfection and decreasing to background levels by approximately 3 h postinfection (Fig. 7). The period of enhancement of infectivity observed upon disruption of microfilaments correlates with that of colocalization of the virus with actin at the cell periphery. OGPy also appears to colocalize with jas-stabilized actin over the time period when this drug inhibits infectivity (Fig. 4). Although the levels of colocalization with actin in jas-treated cells were lower than those in lat A-treated cells, they were higher than the levels in the control (Fig. 7).

DISCUSSION

The polyomaviruses SV40, JCV, and Py depend on different endocytic pathways to infect their respective host cells. SV40 utilizes caveolae (1, 33, 44), and JCV utilizes clathrin-coated vesicles (34). Py is able to enter at least some mouse cells by a pathway that depends neither on caveolae nor clathrin (11). Infection of primary BMK epithelial cells and established fibroblasts (NIH 3T3) by Py is insensitive to disruption of caveolar function by treatment with either cholesterol-binding (MβCD) or -depleting (nystatin) agents. SV40 infection of the same cells is inhibited by these treatments (Table 1). These findings strongly suggest that uptake of these two related viruses in the same cells follows different pathways as dictated by the virus. Alternatively, but less likely, Py and SV40 may utilize a common caveola-dependent pathway but differ quantitatively in their sensitivity to the drugs. These results stand in contrast to those with other mouse cell lines in which Py infectivity was found to be significantly inhibited by treatment with MβCD (36). Different host cells may differ in their susceptibilities to different cholesterol-binding drugs used to assess caveolar function and virus uptake. It is also possible that the same virus may utilize different cellular pathways for uptake in different cells.

Directed trafficking of virus, free or membrane bound, most likely involves cytoskeletal elements (35, 43). The process of trafficking may vary considerably between different viruses of the same or related groups (18). Bovine papillomavirus requires both actin and tubulin for infectivity (51). Adenovirus is taken up into cells via receptor-mediated endocytosis, and after penetration of the endosomal membrane, the viral core particles released into the cytoplasm use microtubules to reach the nucleus, where they enter through the nuclear pore (7, 29, 46). In cells where microtubules have been disrupted, the movement of adenovirus particles containing green fluorescent protein-labeled genomes to the nucleus appears to be via a compensatory mechanism that is microtubule independent (12). The cell type can also influence the mechanism by which the same virus enters and traffics within different cells. Ecotropic murine leukemia virus uses the actin cytoskeleton in both NIH 3T3 and XC cells, but only in XC cells are microtubules also required (19).

Although different polyomaviruses are taken up into cells by different endocytic pathways, once inside the cell these viruses

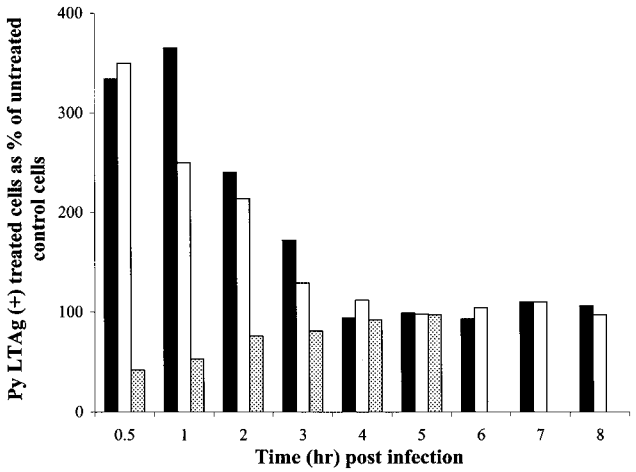

FIG. 5. Effect of actin binding compounds on NIH 3T3 cells. NIH 3T3 cells were pretreated with media alone or media containing either lat A (white bars), cyto B (black bars), or jas (dotted bars). Cells were infected with Py (at an MOI of 10) for 1 h in media alone or media containing the above compounds. The compounds were washed out, and neutralizing antibody was added at the indicated time points. Cells were examined for Py LTAg staining at 32 h. Approximately 500 nuclei were counted per sample, and the data are presented as described in the legend to Fig. 1.

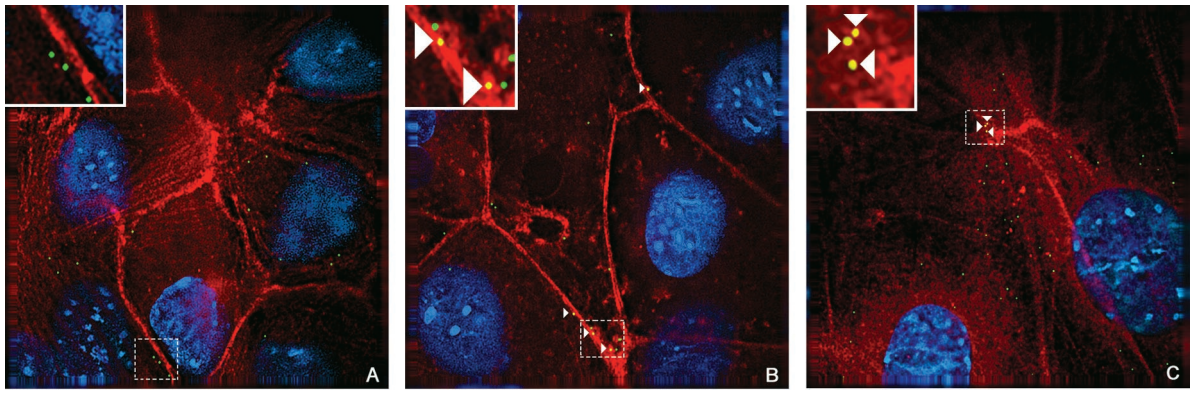

FIG. 6. Colocalization of OGPy with actin. BMK cells were mock treated or pretreated with lat A or jas. Cells were infected with OGPy in the presence or absence of compounds and then further incubated in media alone (A) or with lat A (B) or jas (C). Cells were fixed, processed for immunofluorescence, imaged, and then subjected to deconvolution. Z sections (0.2 μm thick) were examined, and representative ones showing cells that were incubated for 30 min at 37°C prior to fixation are presented. Colocalized OGPy particles are indicated with white arrowheads.

all traffic to the nucleus as the common site of viral replication (5, 13, 24, 26). There is evidence that SV40 particles enter the cytoplasm prior to entering the nucleus via the nuclear pore (5, 50). In view of their size (45 to 50 nm), these viruses could freely diffuse within the cytoplasm to the nuclear periphery but would have to undergo disassembly in order to enter the nucleus via the nuclear pore. Partial uncoating of viral particles in the ER or other membrane-bound compartment may also occur, as recently described for SV40 (31). It is unclear how SV40 or Py would penetrate such a compartment, although a role of VP2 myristylation has been suggested for Py (21, 37).

Our findings on the requirement for intact microtubules are in agreement with earlier work of others on both Py (20, 36) and SV40 (39). The requirement for intact microtubules in Py infectivity appears to be early, as disruption with Colcemid after 8 h no longer has any effect on infectivity. Microtubules are not required for the uptake of Py from the cell surface, as there is no difference in the kinetics or efficiency of escape from neutralization with or without intact microtubules. The block to infectivity by Colcemid is complete even with a high MOI. Intact microtubules are required for a postpenetration step of the life cycle, presumably trafficking of the particles, free or in vesicles, to the nucleus or some other intracellular destination. The colocalization of OGPy and intact microtubules is maximal between 2 and 4 h postinfection (Fig. 2), approximately midway through the period of Colcemid sensitivity, as expected. Two factors may contribute to the number of particles associated with microtubules being less than 100%: (i) the infectious-to-physical particle ratio of less than one and (ii) the inherent asynchrony of infection leading to OGPy particles not being identically aligned along the entry pathway at any given time. The microtubule-dependent step in SV40, which occurs between 3 and 6 h postinfection, is required for the transfer of SV40 between the caveosome and the smooth ER-derived tubules (32). The microtubule-dependent step in the Py infectious pathway may reflect an analogous transfer process. Thus far, we have not observed OGPy particles accumulating in any particular location or compartment in untreated or Colcemid-treated cells through the first 5 to 8 h postinfection, as has been reported for SV40 and Py (32, 36). This is due most likely to the fact that the total number of particles per cell used in our experiments is 1 to 2 orders of magnitude lower than those used by other investigators.

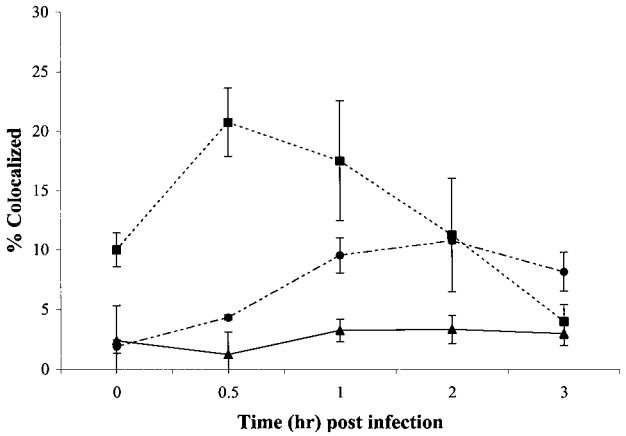

FIG. 7. Quantitation of colocalization of actin and OGPy. BMK cells were mock treated (▲) or pretreated with lat A (■) or jas (●) and then infected with OGPy in the presence or absence of these compounds. Samples were fixed and processed for the detection of actin. After deconvolution, each individual 0.2-μm-thick Z section was examined for number of total virus particles and number of particles colocalized with actin. The averages of three randomly selected fields from three experiments were taken for each time point.

Disruption of the actin cytoskeletal network prior to infection enhances Py infectivity in both epithelial cells and fibroblasts (Table 3). The enhancement is saturable, i.e., only at lower MOIs (≤20 PFU/cell) is enhancement observed. The saturability of the actin disruption effect could suggest the presence of a cellular factor(s), possibly an actin-binding protein released from its normal role in actin-dependent endocytosis, which is limiting both for the enhancement effect and for infectivity under normal conditions. It could also indicate that at higher MOIs, where enhancement is not observed, a secondary endocytic pathway that results in a successful infection could be employed. The ability of a virus to use multiple pathways to enter cells has been recently described for influenza virus (40). Influenza virus infectivity is dependent upon

the virus encountering a compartment with an acidic pH (42), presumably via clathrin-mediated endocytosis as the primary route (25). Disruption of the canonical endocytic pathways (clathrin- and caveola-mediated) did not inhibit the ability of influenza to infect cells (40). Interestingly, influenza uses sialic acid as the primary receptor, similar to murine Py. The relative lack of specificity of sialic acid as a primary receptor for a specific endocytic route may contribute to the use of alternative endocytic pathways.

The enhancement effect of Py infectivity by actin-disrupting drugs occurs during the first 3 h postinfection. One hypothesis is that disruption of the actin cytoskeleton causes redistribution of a viral receptor. However, disruption of the actin cytoskeleton does not appear to cause redistribution of virus receptors from the cell surface to regions of disrupted actin in uninfected cells, as judged by the absence of colocalization of actin with the lectin *Maackia amurensis*, which binds to cell-surface α-2,3-linked sialic acid residues (data not shown). A subset of α-2,3-linked sialic acid-containing proteins that serve as receptors for Py may relocalize upon treatment of cells and remain undetected. The possibility that the Py particles are transferred from α-2,3-linked sialic acid containing primary receptors to putative secondary receptors that can relocalize upon disruption of actin filaments cannot be ruled out. There is currently no evidence of a secondary receptor for Py, and attempts to identify a unique sialic acid-containing primary receptor have not been successful (3)

A second hypothesis is that the effect of these actin-disrupting agents may simply be to clear the cell periphery of the dense network of cortical actin filaments, thereby facilitating further penetration into the cytoplasm by vesicles containing virus. However, OGPy is seen to colocalize with actin in drug-treated, but not untreated, cells, and the kinetics of colocalization correspond well with the period of enhancement of infectivity by the drugs. These observations suggest that it may not simply be the diminution of cortical actin filaments that enhances Py infectivity.

A dynamic state of the actin cytoskeleton at the cell periphery appears to enhance the primary endocytic pathway used by Py for entry. Cells treated with actin-disrupting compounds are more efficient for virus uptake, as evidenced by resistance of virus to neutralization. The interaction between OGPy and actin in treated cells may occur at the cell surface or just after the particles are taken up into vesicles. Colocalization of virus and actin may reflect a functional association of virus with dynamic sites of actin polymerization and depolymerization or possibly interaction with some actin-binding protein(s) that colocalizes with actin patches in cells treated with actin-disrupting agents. The effect of jas, which stabilizes filaments by blocking barbed-end depolymerization, in inhibiting Py infection is also consistent with a role of a dynamic state of the microfilament system in uptake and trafficking of Py. How the localization and clustering of virus at actin patches leads to more-efficient endocytosis of the particles is not known. There is precedence for both enhanced endocytosis (9, 22) and enhanced entry of other pathogens (16, 30) upon actin disruption.

Interestingly, SV40 uptake was not enhanced by disruption of the actin cytoskeleton, although global rearrangement of actin stress fibers, coupled to a tyrosine kinase activity, did accompany virus uptake (33). Richterova et al. (36) reported a similar rearrangement of actin upon Py infection. Thus far, we have not observed a comparable degree of rearrangement of the actin cytoskeleton using OGPy at 50 to 200 particles per cell or unlabeled Py at an MOI of 1,500. This may reflect differences in the specific endocytic pathways these viruses use to enter cells. SV40 enters cells in a caveola- and dynamin-dependent fashion, whereas Py entry is insensitive to caveola disruption and dynamin independent (11) in NIH 3T3 and BMK cells. It remains to be seen if the role of actin dynamics in the infectivity of these two related viruses reflects a common step following penetration or two divergent mechanisms that both rely on actin.

ACKNOWLEDGMENTS

This work has been supported by grants R35-44343, R01 CA 082395, and PO1-50661 from the National Cancer Institute (NCI). J.M.G. has been supported by NCI training grant 2T32-CA72320 and is a recipient of a Bunting fellowship from the Radcliffe Institute for Advance Studies at Harvard University.

We acknowledge the technical assistance of Rebecca Dowgiert and John Carroll and useful discussions with Lan Bo Chen, Stephen Harrison, and Peter Sorger.

REFERENCES

1. **Anderson, H. A., Y. Chen, and L. C. Norkin.** 1996. Bound simian virus 40 translocates to caveolin-enriched membrane domains and its entry is inhibited by drugs that selectively disrupt caveolae. Mol. Biol. Cell **7:**1825–1834.
2. **Atwood, W. J., and L. C. Norkin.** 1989. Class I major histocompatibility proteins as cell surface receptors for simian virus 40. J. Virol. **63:**4474–4477.
3. **Bauer, P. H., C. Cui, T. Stehle, S. C. Harrison, J. A. DeCaprio, and T. L. Benjamin.** 1999. Discrimination between sialic acid-containing receptors and pseudoreceptors regulates polyomavirus spread in the mouse. J. Virol. **73:**5826–5832.
4. **Chen, M., and T. Benjamin.** 1997. Roles of N-glycans with α-2,6 as well as α-2,3 linked sialic acid in infection by polyoma virus. Virology **233:**400–442.
5. **Clever, J., M. Yamada, and H. Kasamatsu.** 1991. Import of simian virus 40 virions through nuclear pore complexes. Proc. Natl. Acad. Sci. USA **88:**7333–7337.
6. **Consigli, R. A., J. Zabielski, and R. Weil.** 1973. Plaque assay of polyoma virus in primary mouse kidney cell cultures. Appl. Microbiol. **26:**627–628.
7. **Dales, S., and Y. Chardonnet.** 1973. Early events in the interaction of adenoviruses with HeLa cells. IV. Association with microtubules and the nuclear pore complex during vectorial movement of the inoculum. Virology **56:**465–483.
8. **Dawe, C. J., R. Freund, G. Mandel, K. Ballmer-Hofer, D. A. Talmage, and T. L. Benjamin.** 1987. Variations in polyoma virus genotype in relation to tumor induction in mice. Characterization of wild type strains with widely differing tumor profiles. Am. J. Pathol. **127:**243–261.
9. **Ellinger, I., A. Rothe, M. Grill, and R. Fuchs.** 2001. Apical to basolateral transcytosis and apical recycling of immunoglobulin G in trophoblast-derived BeWo cells: effects of low temperature, nocodazole, and cytochalasin D. Exp. Cell Res. **269:**322–331.
10. **Fried, H., L. D. Cahan, and J. C. Paulson.** 1981. Polyoma virus recognizes specific sialyloligosaccharide receptors on host cells. Virology **109:**188–192.
11. **Gilbert, J. M., and T. L. Benjamin.** 2000. Early steps of polyomavirus entry into cells. J. Virol. **74:**8582–8588.
12. **Glotzer, J., A. Michou, A. Baker, M. Saltik, and M. Cotten.** 2001. Microtubule-independent motility and nuclear targeting of adenoviruses with fluorescently labeled genomes. J. Virol. **75:**2421–2434.
13. **Griffith, G. R., S. J. Marriott, D. A. Rintoul, and R. A. Consigli.** 1988. Early events in polyomavirus infection: fusion of monopinocytotic vesicles containing virions with mouse kidney cell nuclei. Virus Res. **10:**41–52.
14. **Herrmann, M., C. W. von der Lieth, P. Stehling, W. Reutter, and M. Pawlita.** 1997. Consequences of a subtle sialic acid modification on the murine polyomavirus receptor. J. Virol. **71:**5922–5931.
15. **Hummeler, K., N. Tomassini, and F. Sokol.** 1970. Morphological aspects of the uptake of simian virus 40 by permissive cells. J. Virol. **6:**87–93.
16. **Jones, N. L., J. C. Lewis, and B. A. Kilpatrick.** 1986. Cytoskeletal disruption during human cytomegalovirus infection of human lung fibroblasts. Eur. J. Cell Biol. **41:**304–312.
17. **Kartenbeck, J., H. Stukenbrok, and A. Helenius.** 1989. Endocytosis of simian virus 40 into the endoplasmic reticulum. J. Cell Biol. **109:**2721–2729.
18. **Kasamatsu, H., and A. Nakanishi.** 1998. How do animal DNA viruses get to the nucleus? Annu. Rev. Microbiol. **52:**627–686.

19. **Kizhatil, K., and L. M. Albritton.** 1997. Requirements for different components of the host cell cytoskeleton distinguish ecotropic murine leukemia virus entry via endocytosis from entry via surface fusion. J. Virol. **71:**7145–7156.
20. **Krauzewicz, N., J. Stokrova, C. Jenkinds, M. Elliott, C. F. Higgins, and B. E. Griffin.** 2000. Virus-like gene transfer into cells mediated by polyoma virus pseudocapsids. Gene Ther. **7:**2122–2131.
21. **Krauzewicz, N., C. H. Streuli, N. Stuart-Smith, M. D. Jones, S. Wallace, and B. E. Griffin.** 1990. Myristylated polyomavirus VP2: role in the life cycle of the virus. J. Virol. **62:**4414–4420.
22. **Lewis, C. M., A. K. Smith, and B. A. Kamen.** 1998. Receptor-mediated folate uptake is positively regulated by disruption of the actin cytoskeleton. Cancer Res. **58:**2952–2956.
23. **Liu, C. K., G. Wei, and W. J. Atwood.** 1998. Infection of glial cells by human polyomavirus JC is mediated by an N-linked glycoprotein containing terminal a(2–6)-linked sialic acids. J. Virol. **72:**4643–4649.
24. **MacKay, R. L., and R. A. Consigli.** 1976. Early events in polyoma virus infection: attachment, penetration, and nuclear entry. J. Virol. **19:**620–636.
25. **Marsh, M., and A. Helenius.** 1989. Virus entry into animal cells. Adv. Virus Res. **36:**107–151.
26. **Mattern, C. F. T., K. K. Takemoto, and W. A. Daniel.** 1966. Replication of polyoma virus in mouse embryo cells: electron microscopic observations. Virology **30:**242–256.
27. **Maul, G. G., G. Rovera, A. Vorbrodt, and J. Abramczuk.** 1978. Membrane fusion as a mechanism of simian virus 40 entry into different cellular compartments. J. Virol. **28:**936–944.
28. **McMillen, J., and R. A. Consigli.** 1977. Immunological reactivity of antisera to sodium dodecyl sulfate-derived polypeptides of polyoma virions. J. Virol. **21:**1113–1120.
29. **Miles, B. D., R. B. Luftig, J. A. Weatherbee, R. R. Weihing, and J. Weber.** 1980. Quantitation of the interaction between adenovirus types 2 and 5 and microtubules inside infected cells. Virology **105:**265–269.
30. **Murai, M., K. Seki, J. Sakurada, A. Usui, and S. Masuda.** 1993. Effects of cytochalasins B and D on Staphylococcus aureus adherence to and ingestion by mouse renal cells from primary culture. Microbiol. Immunol. **37:**69–73.
31. **Norkin, L. C., H. A. Anderson, S. A. Wolfrom, and A. Oppenheim.** 2002. Caveolar endocytosis of simian virus 40 is followed by brefeldin A-sensitive transport to the endoplasmic reticulum, where the virus disassembles. J. Virol. **76:**5156–5166.
32. **Pelkmans, L., J. Kartenbeck, and A. Helenius.** 2001. Caveolar endocytosis of simian virus 40 reveals a new two-step vesicular-transport pathway to the ER. Nat. Cell Biol. **3:**473–483.
33. **Pelkmans, L., D. Puntener, and A. Helenius.** 2002. Local actin polymerization and dynamin recruitment in SV40-induced internalization of caveolae. Science **296:**535–539.
34. **Pho, M. T., A. Ashok, and W. J. Atwood.** 2000. JC virus enters human glial cells by clathrin-dependent receptor-mediated endocytosis. J. Virol. **74:**2288–2292.
35. **Provance, D. W., A. McDowall, M. Marko, and K. Luby-Phelps.** 1993. Cytoarchitecture of size-excluding compartments in living cells. J. Cell Sci. **106:**565–577.
36. **Richterova, Z., D. Liebl, M. Horak, Z. Palkova, J. Stokrova, P. Hozak, J. Korb, and J. Forstova.** 2001. Caveolae are involved in the trafficking of mouse polyomavirus virions and artificial VP1 pseudocapsids toward cell nuclei. J. Virol. **75:**10880–10891.
37. **Sahli, R., R. Freund, T. Dubensky, R. Garcea, R. Bronson, and T. Benjamin.** 1993. Defect in entry and altered pathogenicity of a polyoma virus mutant blocked in VP2 myristylation. Virology **192:**142–153.
38. **Sanjuan, N., M. Zijlstra, J. Carroll, R. Jaenisch, and T. Benjamin.** 1992. Infection by polyomavirus of murine cells deficient in class I major histocompatibility complex expression. J. Virol. **66:**4587–4590.
39. **Shimura, H., Y. Umeno, and G. Kimura.** 1987. Effects of inhibitors of the cytoplasmic structure and functions on the early phase of infection of cultured cells with simian virus 40. Virology **158:**34–43.
40. **Sieczkarski, S. B., and G. R. Whittaker.** 2002. Influenza virus can enter and infect cells in the absence of clathrin-mediated endocytosis. J. Virol. **76:**10455–10464.
41. **Simons, K., and D. Toomre.** 2000. Lipid rafts and signal transduction. Nat. Rev. Mol. Cell Biol. **1:**31–40.
42. **Skehel, J. J., T. Bizebard, P. A. Bullough, F. M. Hughson, M. Knossow, D. A. Steinhauer, S. A. Wharton, and D. C. Wiley.** 1995. Membrane fusion by influenza virus. Cold Spring Harbor Symp. Quant. Biol. **55:**573–580.
43. **Sodeik, B.** 2000. Mechanisms of viral transport in the cytoplasm. Trends Microbiol. **8:**465–472.
44. **Stang, E., J. Kartenbeck, and R. G. Parton.** 1997. Major histocompatibility complex class I molecules mediate association of SV40 with caveolae. Mol. Biol. Cell **8:**47–57.
45. **Stehle, T., and S. C. Harrison.** 1997. High-resolution structure of a polyomavirus VP1-oligoaccharide complex: implications for assembly and receptor binding. EMBO J. **16:**5139–5148.
46. **Suomalainen, M., M. Nakano, S. Keller, K. Boucke, R. Stidwill, and U. Greber.** 1999. Microtubule-dependent plus and minus end-directed motilities are competing processes for nuclear targeting of adenovirus. J. Cell Biol. **144:**657–672.
47. **Suzuki, S., H. Sawa, R. Komagome, Y. Orba, M. Yamada, Y. Okada, Y. Ishida, H. Nishihara, S. Tanaka, and K. Nagashima.** 2001. Broad distribution of the JC virus receptor contrasts with a marked cellular restriction of virus replication. Virology **286:**100–112.
48. **Wallace, W., L. H. Schaefer, and J. R. Swedlow.** 2001. A workingperson's guide to deconvolution in light microscopy. BioTechniques **31:**1076–1097.
49. **Wei, G., C. K. Liu, and W. J. Atwood.** 2000. JC virus binds to primary human glial cells, tonsillar stromal cells, and B-lymphocytes, but not to T lymphocytes. J. Neurovirol. **6:**127–136.
50. **Yamada, M., and H. Kasamatsu.** 1993. Role of nuclear pore complex in simian virus 40 nuclear targeting. J. Virol. **67:**119–130.
51. **Zhou, J., L. Gissmann, H. Sentgraf, H. Muller, M. Picken, and M. Muller.** 1995. Early phase in the infection of cultured cells with papillomavirus virions. Virology **214:**167–176.